Journal of Manufacturing Engineering, September 2026, Vol. 21, Issue. 3, pp 117-128
DOI. https://doi.org/10.37255/jme.v21i3pp117-128

THEORETICAL AND EXPERIMENTAL STUDY ON DYNAMIC MINIMUM CUTTING THICKNESS

Wang Jianping, Han Bin, Kuai Jicai, Duan Yunqian, Dmitrii V. Ardashev

Henan Polytechnic University, School of Mechanical and Power Engineering, Jiaozuo 454000
South Ural State University, Russia

Abstract

The cutting thickness has a significant impact on surface quality: the thinner the cutting thickness, the easier it is to achieve good surface quality. The minimum cutting thickness represents the limit for chip formation. Theoretically, performing ultra-precision cutting at the minimum cutting thickness enables the achievement of an excellent machined surface with minimal surface damage and exceptional surface quality. Therefore, exploring the formation mechanism of the minimum cutting thickness and investigating the formation mechanism of surface micro topography under extreme cutting conditions are of great significance for further clarifying the extreme cutting theory, improving surface quality, and extending tool life. A dynamic minimum cutting thickness theory is proposed, followed by calculations and simulations. Furthermore, scratch experiments on aluminum alloys and red copper are conducted using a single-crystal diamond tool, during which the cutting force and scratch depth are measured. The minimum cutting thickness of aluminum alloys and red copper is determined by leveraging the corresponding relationship between the abrupt change in cutting force (from the plowing stage to the cutting stage) and the scratch depth. Based on the minimum cutting thickness, the optimal cutting parameters for the non-free cutting of aluminum alloys and red copper were obtained, and non-free cutting experiments were conducted using these parameters. The results show that the minimum cutting thickness of aluminum alloys and red copper increases with increasing feed rate. The ratios of the minimum cutting thickness to the tool edge radius are in the ranges of 0.243–0.271 and 0.20–0.36, respectively. The optimal surface roughness values are as follows: Rz = 1.505 μm and 2.014 μm, and Ra = 0.293 μm and 0.309 μm, respectively.

Keywords. *Dynamic minimum cutting thickness, super-precision cutting, single-crystal diamond tool*

1. Introduction

The thinner the chip, the more precise the cutting process, and the easier it is to obtain a machined surface with high precision. As the cutting thickness approaches the minimum, the surface quality tends to be optimal. Thus, the influencing factors of the minimum cutting thickness and its realization methods have long been the focus of extensive attention among researchers.

In 1987, Osaka University (Japan) and the LLL Laboratory (USA) conducted research on the limits of ultra-precision machining. One of the key achievements was the study of the minimum cutting thickness, with a chip thickness of 1 nm obtained using an extremely sharp single-crystal diamond tool under strict cutting conditions [1]. To date, this research still represents the limit of ultra-precision machining and has not been surpassed. Subsequently, they investigated the minimum cutting thickness and its influencing factors using molecular dynamics simulations, concluding that it is 5% of the tool edge radius [2]. In their research on cutting aluminum alloy materials with diamond tools, Yuan Zhejun et al. indicated that the minimum cutting thickness is influenced by the tool edge radius, material properties, and the cutting process, and that the resulting minimum cutting thickness is approximately 20%–40% of the tool edge radius [3]. Son Seong Min conducted research on the relationship between the minimum cutting thickness and the friction coefficient between the tool and the workpiece by machining aluminum, brass, and oxygen-free high-conductivity copper with a single-crystal diamond tool. The results showed that the tool edge radius and the friction coefficient between the tool and the workpiece are the main influencing factors of the minimum cutting thickness in the micro-cutting process; a smaller edge radius and a larger friction coefficient can lead to thinner chips. The minimum cutting thickness of the three materials ranges from 0.09 to 0.12 μm, and the ratio of the minimum cutting thickness to the tool edge

**Corresponding Author -E-mail: 1553616465@qq.com*

radius (r_n = 0.5 μm) is 18%–24% [4]. In 2010, H.L. Zhang studied the minimum cutting thickness of copper and aluminum using an atomic force microscope [5].In 2018, Zhichao Niu et al. conducted micro-cutting experiments on 6082-T6 aluminum alloy using diamond and WC tools. The research showed that before chip formation, the plowing effect was significant and the normal force was relatively large; however, when chips began to form, the tangential force exceeded the normal force. Based on this observation, the minimum cutting thickness of aluminum alloy 6082-T6 was determined to be 0.2–0.3 μm, and the ratio of the minimum cutting thickness to the tool edge radius (1.4 μm) was approximately 14%–21% [6].In 2020, Xian Wu et al. proposed a micro-cutting effective rake angle model, determined that the ratio of the minimum cutting thickness of copper to the tool-edge radius was 0.17, and verified this by cutting electrolytic tough pitch copper T2 with TiCN-coated WC tools [7].In 2018, Zhenyu Shi et al. studied the minimum undeformed cutting thickness of Inconel 718 using acoustic emission technology and finite-element simulation. They used a micro-milling cutter with a 6 μm edge radius to machine Inconel 718. The results showed that the minimum cutting thickness was 1.41 μm, and the ratio of the minimum cutting thickness to the edge radius was 0.23 [8]. The aforementioned research findings indicate that the minimum cutting thickness is closely related to tool geometry and friction coefficient [9], and is influenced by factors such as changes in tool geometry caused by tool wear during the cutting process [10], changes in material properties induced by cutting heat and other factors [11], and variations in process parameters [12].

In 1996, W. Grzesik studied the minimum cutting thickness and its influence on surface roughness based on the Kragelskii-Drujanov model 1. The research indicates that as the feed rate increases, both the minimum cutting thickness and the surface roughness increase [13]. In 2006, X. Liu conducted research on the minimum-cutting-thickness model and micro-cutting conditions. The research shows that the minimum cutting thickness increases with increasing tool edge radius and cutting speed [14].In 2007, T. Özel et al. studied the variation in the minimum cutting thickness with tool edge radius and cutting speed while machining AL 2024-T6 and AISI 4340 using a micro-milling cutter. The results showed that the minimum cutting thickness increases with increasing tool edge radius and cutting speed [15]. In 2012, M. Malekian et al. proposed a minimum-cutting-thickness neutral-angle model1. They used the principle of minimum energy to calculate that the neutral angle is approximately equal to the friction angle. They cut Al6061 with a WC tool (with a tool-edge radius of 13μm), measured the force ratio to be about 0.8, and then calculated the friction angle to be 39, that is, the neutral angle is 39. From this, the minimum cutting thickness for Al6061 was determined to be 0.23 m. They believed that the minimum cutting thickness is closely related to tool geometry and material properties, and that it increases with increasing friction coefficient [16].In 2012, A. Cuba Ramos et al. conducted ramp-cutting groove experiments and measured the variation in groove roughness. They proposed that the groove position with a drastic change in roughness is where the minimum cutting thickness occurs; the corresponding scratch depth at this position is then taken as the minimum cutting thickness. Their research indicated that the minimum cutting thickness decreases with increasing cutting speed and increases with increasing tool edge radius [17]. In 2017, Przestacki, D. et al. performed cutting experiments on WC/NiCr coatings using laser-assisted PCD tools (with a tool edge radius of r_n = 7.1 μm). They found that when the cutting speed increased from 10 to 30 m/min, the minimum cutting thickness ranged from 1.1 to 1.8 μm [18]. In 2018, Hamed Rezaei et al. processed Ti-6Al-4V with WC end mills (edge radius rn = 6.089±0.234 μm) and studied the minimum cutting thickness under different cooling environments 1. The research showed that in the case of dry cutting, the minimum cutting thickness of Ti-6Al-4V was 1.5 - 3.0μm (0.25–0.49r_n), and under the minimum quantity lubrication (MQL) cooling condition, the minimum cutting thickness of Ti-6Al-4V decreased to 0.9 - 2.1μm (0.15–0.34rn). The analysis suggests that this phenomenon is attributed to the coolant reducing tool wear and minimizing built-up edges. The research also indicates that cutting depth and cutting speed have no significant impact on the minimum cutting thickness [19].In 2019, W. S. Yip et al. conducted magnetically assisted ultra-precision cutting of Ti6Al4V titanium alloy to investigate the effect of the magnetic field on the minimum cutting thickness. The results showed that under the action of the magnetic field, the friction coefficient between the tool and the workpiece increased significantly, and the minimum cutting thickness decreased by 50% [20]. In 2020-2023, Mikoajczyk T et al. studied the influence of the inclination angle of the bevel cutting edge on the minimum cutting thickness. They believed that the minimum cutting thickness decreases with increasing inclination angle, which provides a new research direction for the tool structure in precision cutting [21, 22].

In 2021, Yiquan Li et al. established a neutral-angle model for the minimum cutting thickness and calculated it using the minimum-energy principle. They believed that as fracture toughness increased, the shear

Journal of Manufacturing Engineering, September 2026, Vol. 21, Issue. 3, pp 117-128
DOI. https://doi.org/10.37255/jme.v21i3pp117-128

angle decreased, the neutral angle increased, and thus the minimum cutting thickness increased. Additionally, the minimum cutting thickness increased with increasing undeformed chip thickness [23].

The aforementioned research has pioneered the theory of dynamic minimum cutting thickness, showing that the minimum cutting thickness depends on actual cutting parameters and varies with changes in tool edge radius, cutting parameters, and workpiece material properties. Therefore, following the "research on the limits of ultra-precision machining conducted by Osaka University (Japan), this research has achieved a new breakthrough in the limits of ultra-precision machining. However, this research is limited to specific materials. Researchers have reached a consensus that the minimum cutting thickness is related to tool geometry and material properties, but there are divergent views on the specific mechanisms of influence. For instance, Son Seong Min et al. argued that the minimum cutting thickness decreases as the friction coefficient increases [4], while M. Malekian put forward the opposite view, believing that the minimum cutting thickness increases as the friction coefficient rises [16]; another example is that T. Özel et al. suggested the minimum cutting thickness increases with an increase in cutting speed [15], whereas A. Cuba Ramos et al. held that the minimum cutting thickness decreases when the cutting speed increases [17]. It can be concluded from this that the law governing the minimum cutting thickness remains unclear. However, the technical key to achieving ultra-precision machining and obtaining a fine surface lies in realizing ultra-stable ultra-precision cutting with extremely thin chips. Therefore, exploring the theory of minimum cutting thickness and its implementation technology is of great significance for advancing ultra-precision machining theory and technology.

Conduct theoretical and experimental research on the minimum cutting thickness. First, it analyzes the statistical distributions of the friction coefficient and the cutting force ratio between the tool and the workpiece during cutting. Then, it explores the effects of the friction coefficient and the cutting force ratio on the minimum cutting thickness and proposes a theory of dynamic minimum cutting thickness. On this basis, it further analyzes the impact of dynamic minimum cutting thickness on surface roughness. Finally, cutting experiments on aluminum alloy and red copper are conducted using a single-crystal diamond tool on a self-developed micro-cutting platform; these experiments aim to study the theory of dynamic minimum cutting thickness and its effect on surface quality, as well as explore the implementation method of ultra-precision machining technology based on dynamic minimum cutting thickness.

2. Theoretical and Experimental Study on Dynamic Minimum Cutting Thickness.

As shown in Fig. 1, which illustrates the relationship between the minimum cutting thickness and the edge radius, point A is the chip separation point. The material above point A forms chips and is removed, while the material below point A is extruded by the edge arc and the flank face, undergoes elastoplastic deformation, and finally forms the machined surface. Based on the force balance relationship at point A shown in the figure, the following formulas are derived [24]:

$$F_N = F_p\cos\theta + F_f\sin\theta \quad (1)$$

$$F_t = F_f\cos\theta - F_p\sin\theta \quad (2)$$

$$F_t = \mu F_N \quad (3)$$

From formulas (1)-(3), we can derive:

$$\tan\theta = \frac{F_f - \mu F_p}{\mu F_f + F_p} \quad (4)$$

According to the geometric relationship shown in Fig. 1:

$$h_{min} = r_n(1-\cos\theta) = r_n\left(1-\frac{1}{\sqrt{1+\tan\theta^2}}\right) \quad (5)$$

After simplification, we obtain:

$$h_{min} = r_n\left[1-\frac{\mu F_f + F_p}{\sqrt{\left(F_f^2+F_p^2\right)\left(1+\mu^2\right)}}\right] \quad (6)$$

Where r_n is the tool edge radius, F_p is the normal force, F_f is the tangential force, and is the friction coefficient.

It can be seen that the minimum cutting thickness is related to the edge radius, the friction coefficient between the tool and the workpiece, and the force ratio. During the cutting process, as the tool wears from a new tool to the passivation standard (before replacement), the friction coefficient and force ratio change in real time with cutting time, the degree of tool passivation, and the degree of softening of the workpiece material under the action of cutting heat. Thus, it is theoretically predicted that the minimum cutting

Journal of Manufacturing Engineering, September 2026, Vol. 21, Issue. 3, pp 117-128
DOI. https.//doi.org/10.37255/jme.v21i3pp117-128

thickness should not be fixed but varies with changes in cutting conditions.

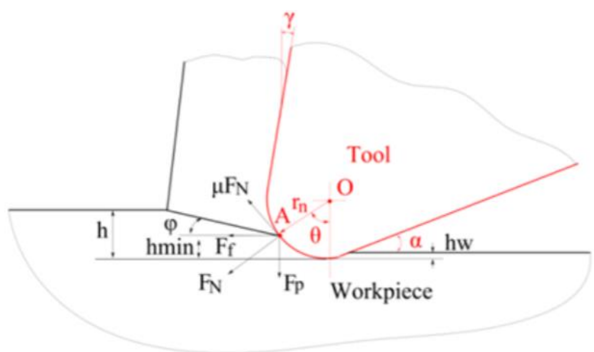

Fig. 1. Schematic Diagram of Minimum Cutting Thickness Analysis

During the cutting process, the tool state is determined, and the edge radius is a constant. If the tool is in the initial state (rn = 10μm), with the friction coefficient and force ratio as variables, the variation law of the minimum cutting thickness with these variables can be obtained, as shown in Fig. 2.

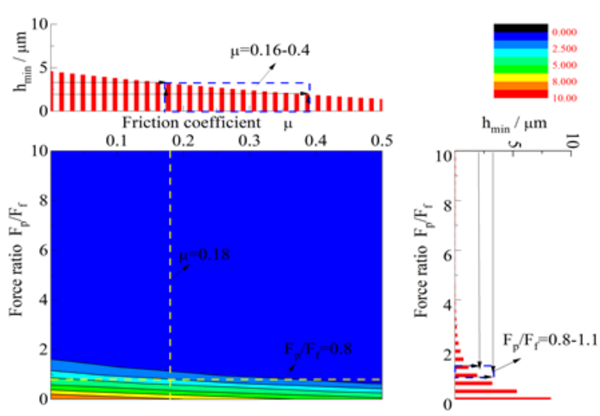

Fig. 2. Variation of Minimum Cutting Thickness with Force Ratio and Friction Coefficient

As shown in Fig. 2, the minimum cutting thickness varies significantly across force ratios from 0 to 2 and friction coefficients from 0 to 0.5. Moreover, it follows a pattern of decreasing as the friction coefficient and force ratio increase. For ultra-precision cutting, the force ratio typically ranges from 0.8 to 1, and the friction coefficient from 0.1 to 0.4. The top-left graph shows how the minimum cutting thickness varies with the friction coefficient at a force ratio of 0.8. It can be observed that the minimum cutting thickness decreases as the friction coefficient increases, but the variation trend is relatively gentle. Within the friction coefficient range of 0.16–0.4, the theoretical values of the minimum cutting thickness vary between 2 and 3.2 μm. The right graph illustrates the change of the minimum cutting thickness with the force ratio when the friction coefficient is 0.18. It is evident that the minimum cutting thickness decreases sharply as the force ratio increases. Within the force ratio range of 0.8–1.1, the theoretical values of the minimum cutting thickness vary from 2.2 to 3.5 μm.

As is known from the minimum cutting thickness theory, the tool divides the surface to be cut into two parts at the chip separation point: one part moves upward along the rake face to form chips, and the other part moves downward along the flank face to form the machined surface. Additionally, the velocity at the chip separation point is zero [16]. Based on the above theory, a cutting simulation of aluminum alloy and red copper using a single-crystal diamond tool was conducted in free-cutting mode using Deform 2D Version 11.0. The simulation parameters were set as follows: diamond tool edge radius of 10 μm, cutting speed of 3000 rpm, and feed rates of 2 μm/r and 3 μm/r, respectively. From the simulation, the cutting velocity distribution diagrams of aluminum alloy and red copper were obtained, as shown in Fig. 3a, 3b, 3c, and 3d.

Fig. 3a shows the cutting velocity distribution diagram at a feed rate of 2 μm/r. As shown in the figure, the minimum cutting thickness at the chip separation point is 2.32 μm. Fig. 3b presents the cutting velocity distribution at a feed rate of 3 μm/r, indicating that the minimum cutting thickness at the chip separation point is 3.2 μm. Taking pure copper as the material, the cutting process was simulated using the above parameters, and the results are shown in Fig. 3c and 3d. As shown in Fig. 3c, the minimum cutting thickness of pure copper at a feed rate of 2 μm/r is 3.7 μm; in Fig. 3d, it reaches 4.3 μm at a feed rate of 3 μm/r. It is evident that the minimum cutting thickness of pure copper is significantly greater than that of the aluminum alloy, which may be due to differences in materials and friction coefficients; however, the simulation used the same friction coefficient for simplification.

From the cutting simulations of aluminum alloy and pure copper, although there are some differences in their minimum cutting thicknesses, both follow the law of increasing minimum cutting thickness with increasing feed rate.

Journal of Manufacturing Engineering, September 2026, Vol. 21, Issue. 3, pp 117-128
DOI. https.//doi.org/10.37255/jme.v21i3pp117-128

3. Experimental Equipment and Principle

3.1. Experimental Principle

As shown in Figure 4, the cutting process is divided into three phases: sliding friction, plowing, and cutting. When the cutting tool contacts the workpiece and slides against it (during the sliding-friction phase), the workpiece undergoes elastic deformation, and the elastic recovery height of the machined surface is h_w. As the cutting depth increases, before chips are generated, plastic deformation occurs on the workpiece surface; this is the plowing stage. When the cutting depth continues to increase and exceeds the minimum cutting thickness h_{min}, chips start to form. The thickness of the chips gradually stabilizes after reaching its minimum value, and this phase is referred to as the cutting stage. The minimum cutting thickness occurs at the transition moment from the plowing stage to the cutting stage. At this point, the cutting mechanism undergoes a transformation, manifested as an abrupt change in cutting force. Measure the cutting force during the transition process from plowing to cutting, and establish a one-to-one correspondence between the cutting force and the cutting process. The position where the minimum cutting thickness occurs can be determined from the location of the abrupt change in cutting force. As shown in Fig. 4, at time t2, the cutting depth reaches the minimum cutting thickness h_{min}; correspondingly, the cutting distance at time t2 is L_2. Therefore, the cutting depth at the position of L_2 equals the minimum cutting thickness.

By combining the position of the abrupt change in cutting force with microscopic observation, the size of the minimum cutting thickness can be determined with relatively high precision.

3.2. Experimental Equipment and Methods:

3.2.1 Experimental Equipment:

The self-built diamond tool cutting test bench is shown in Fig. 5. The test bench's spindle is an electric spindle with a rotational accuracy of 0.001 mm. The feed mechanism combines coarse and fine feeds: the coarse feed is provided by a manual micro-positioning stage with an accuracy of 0.02 mm, while the fine feed is driven by a stepper motor with an accuracy of 0.001 mm. The experimental cutting tool is a single-crystal diamond tool manufactured by Zhengzhou Superhard Tool Co., Ltd., with an edge radius of 10 μm. Fig. 6 shows the SEM test results of the diamond tool. The test pieces used are aluminum alloy and red copper. A model SBT970 dynamometer produced by Guangzhou Sbartor Company is adopted for measurement, with a measuring accuracy of 0.01 N and a measuring range of 0–2 N. For the measurement of surface groove and scratch depth, an ultra-depth-of-field microscope is used.

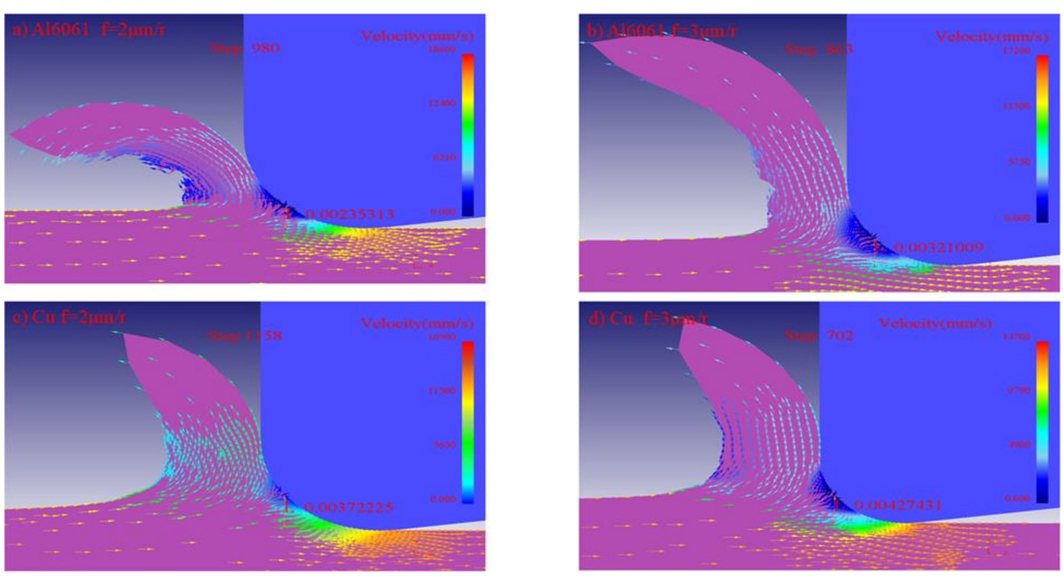

Fig. 3. Cutting Speed Distribution Diagrams of Aluminum Alloy and Pure Copper

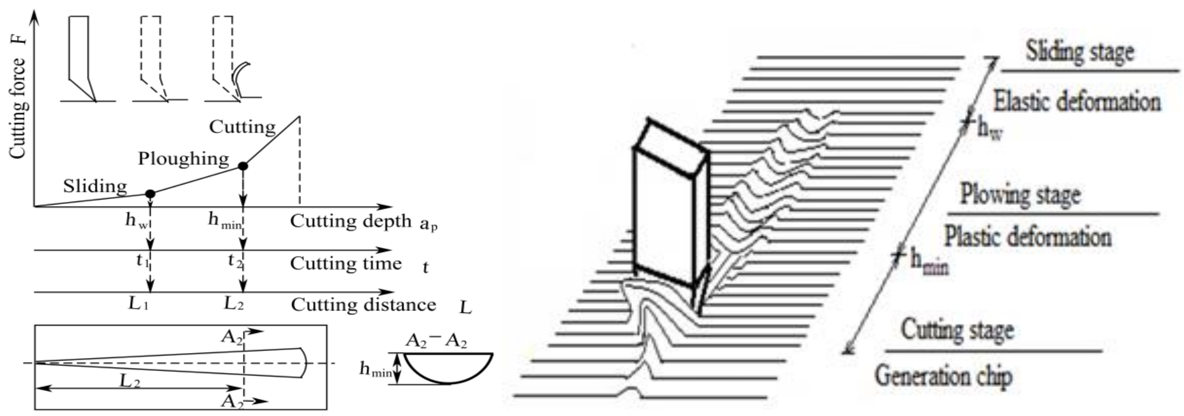

Fig. 4. Experimental principle

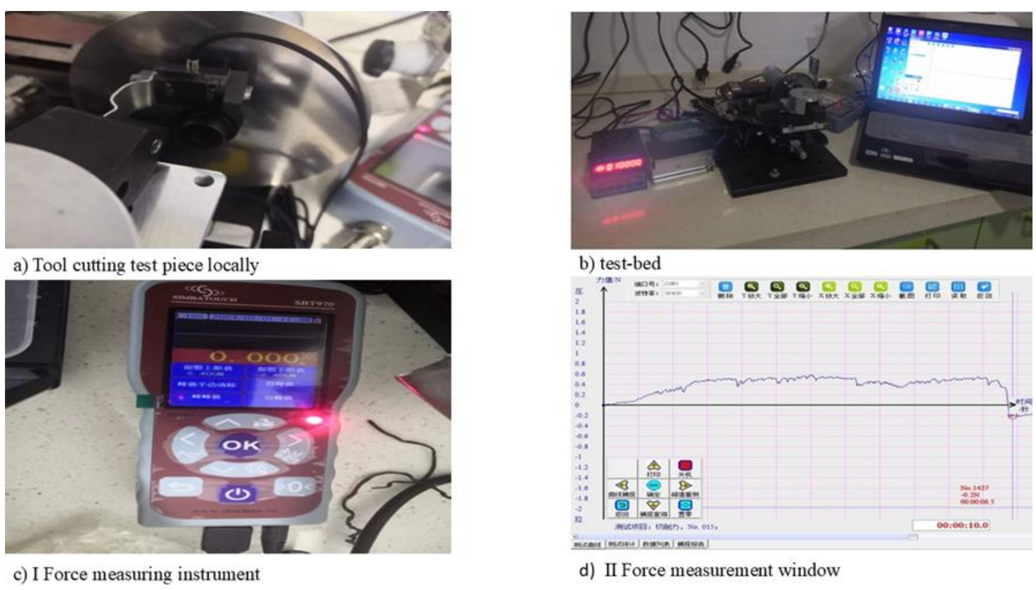

Fig. 5. Experimental Equipment

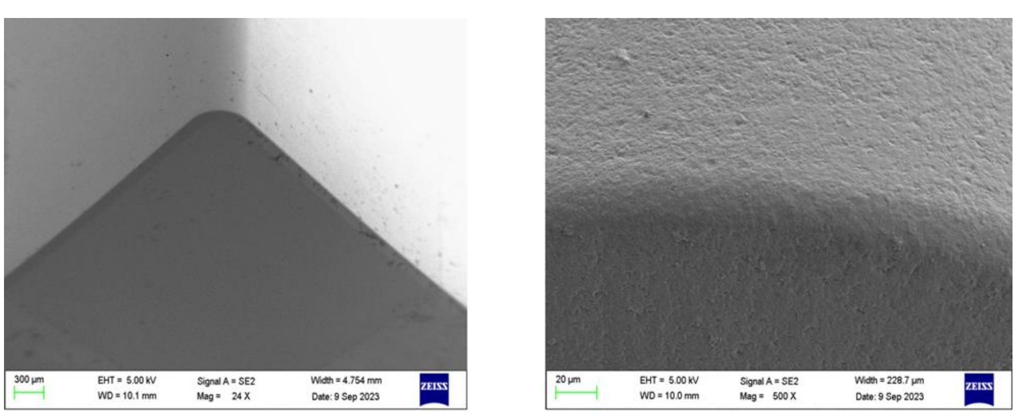

Fig. 6. Diamond Tool

Journal of Manufacturing Engineering, September 2026, Vol. 21, Issue. 3, pp 117-128
DOI. https.//doi.org/10.37255/jme.v21i3pp117-128

Using a diamond cutting tool, continuous variable-depth cutting experiments (from 0 to ap) were conducted on aluminum alloy and red copper at different cutting speeds. Meanwhile, a dynamometer was used to measure the cutting force, and an ultra-depth-of-field microscope was employed to measure the cutting depth at the position where chips are generated on the machined surface, which is the minimum cutting thickness. The experimental parameters are shown in Table 1. The experimental equipment is illustrated in Figure 5. The SEM results for the diamond tool's cutting edge are presented in Figure 6, with an edge radius of 10 μm.

4. Experimental Results and Discussion

4.1. Cutting Force

Fig. 7 shows the variation in cutting force with cutting time during the cutting of aluminum alloy by a diamond tool at feed rates of 1.25 mm/s, 2.5 mm/s, 3.75 mm/s, and 5 mm/s. As shown in Fig. 7a, the cutting force abruptly changes at 1.19 s, corresponding to a cutting distance of 1.49 mm and a theoretical scratch depth of 2.3 μm. From Fig. 7b, it is observed that the cutting force increases sharply at 0.82 s; at this moment, the corresponding cutting distance is 2.05 mm, and the theoretical scratch depth is 3.2 μm. As shown in Fig. 7c, the cutting force rises sharply at 0.59 s, with the corresponding cutting distance being 2.21 mm and the theoretical scratch depth being 3.47 μm. From Fig. 7d, the cutting force increases sharply at 0.45 s, corresponding to a cutting distance of 2.25 mm and a theoretical scratch depth of 3.53 μm.

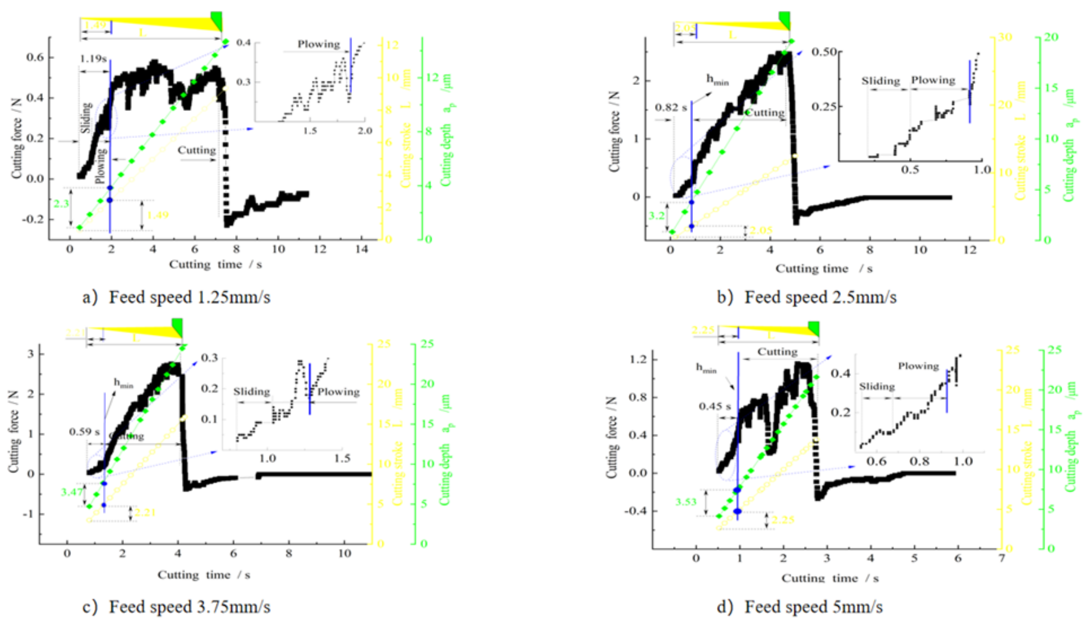

Fig. 7: Measurement Results of Cutting Force at Feed Rates from 1.25 mm/s to 5 mm/s

Table 1 Experimental Parameters

Group		Spindle Speed Vs /m/s	Feed Rate f /mm/s	Cooling Method	Deflection Angle	Tool Fillet Radius rε /mm	Edge Radius rn /μm
1	1-5	0	1.25	无	0.09	0.4	10
2	1-5	0	2.5	无	0.09	0.4	10
3	1-5	0	3.75	无	0.09	0.4	10
4	1-5	0	5	无	0.09	0.4	10

Table 2 Scratch Parameters of Aluminum Alloy and Red Copper

Cutting speed V /mm/s	Al6061			Cu		
	Scratch length L /μm	Scratch width W /μm	Scratch depth a /μm	Scratch length L /μm	Scratch width W /μm	Scratch depth a /μm
1.25	1399.7	80	2.2	1865	93.5	1.975
2.5	2015	130	2.63	2253	95	2.203
3.75	2216	145	2.84	2487	98	2.567
5	2414	120	3.17	3406	105	3.645

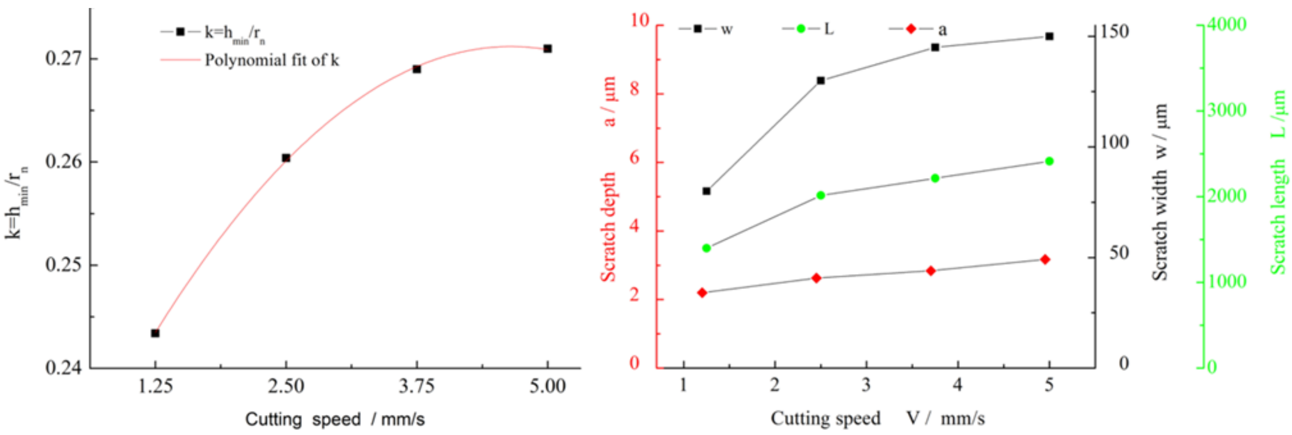

a)The ratio of the minimum cutting thickness to the cutting edge radius

b)Scratch,depth,width,length

Fig. 8. Data analysis of aluminum alloy scratches

4.2. Cutting Scratches

Fig. 9 shows the typical cross-sectional profiles of the scratch positions where chips are generated during the cutting of aluminum alloy by the corresponding diamond tool. The raised end is caused by chip accumulation, and the cross-sectional width and depth of the scratch are measured with the lower end as the reference. The measured data for scratch length, width, and depth for aluminum alloy and red copper are presented in Table 2.

Fig. 8 presents the analysis results for the scratch length, width, and depth of the aluminum alloy at different feed rates. To avoid measurement errors, each data set was measured 5 times, and the average was used as the result shown in Fig. 9. Fig. 9a shows the variation of the ratio k (between the minimum cutting thickness and the edge radius) with the feed rate. As shown in the figure, as the feed rate increases, k gradually increases from 0.243 to 0.271, initially increasing rapidly and then tending toward stability. Fig. 9b shows the variation of scratch depth, width, and length with feed rate. As shown in the figure, when the feed rate increases from 1.25 mm/s to 5 mm/s, the scratch depth ranges from approximately 2 μm to 3 μm and shows a slight upward trend. The scratch width is approximately 80–150 μm, showing a steady increase, while the scratch length is roughly 1300–3400 μm, with the most significant increase.

The scratch analysis of red copper is shown in Fig. 10. To minimize measurement error, the experiment was repeated twice, and each data set was measured 5 times; the average was used as the test result. Figure 10a depicts the variation of the ratio k (between the minimum cutting thickness and the edge radius) with the feed rate. The upper data points represent the first experiment, with a variation range of 0.207–0.439. The lower data points correspond to the second experiment, with a variation range of 0.188–0.29. After fitting the data from the two experiments, the overall variation ranges from 0.188 to 0.29. As the feed rate increases, the ratio k gradually increases. Fig. 10b illustrates the variation of scratch depth, width, and length with feed rate. As can be seen from the figure, with the increase of feed rate, the scratch depth varies in the range of 2–3.5 μm, with an increase rate of nearly 75%; The scratch width changes between

90–110 μm, showing a small increase; The scratch length ranges from 1784 μm to 3666 μm.

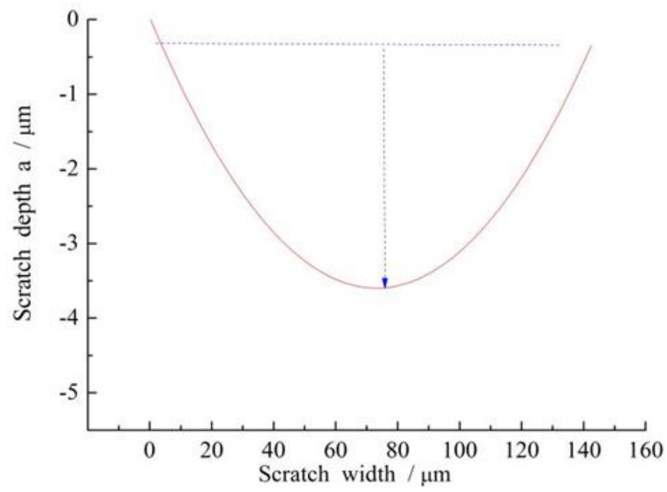

Fig. 9. Ultra-depth-of-field Microscope Test of Cutting Scratches

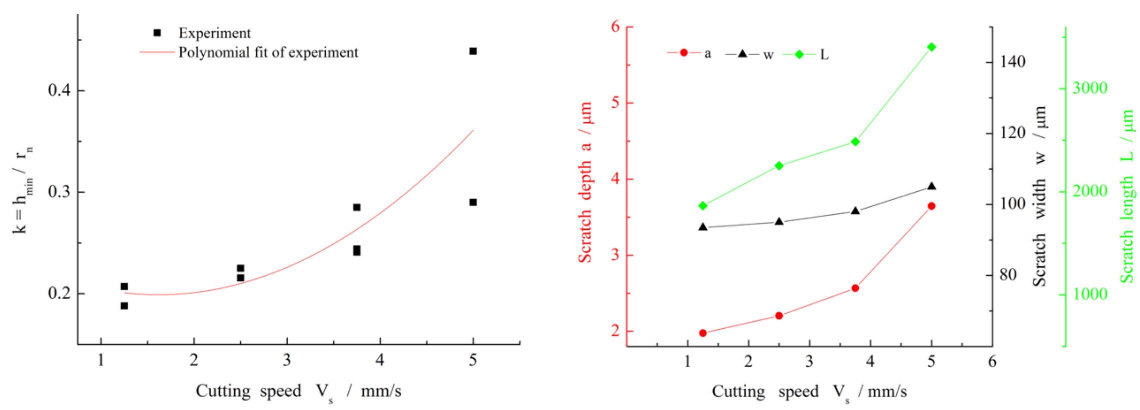

a) The ratio of the minimum cutting thick ness to the cutting edge radius

b) Scratch depth, width, length

Fig.10. Scratch test analysis of copper

The measurement results show that the minimum cutting thicknesses of aluminum alloy and red copper range from 2.2 μm to 3.17 μm and from 2 μm to 3.5 μm, respectively, which are close to the theoretical calculations.

4.3. Surface Roughness

The surface roughness of the workpiece is affected by factors such as specific machining parameters, residual surface height, minimum cutting thickness, elastic recovery, and burr height across different phases. Brammertz considered the influence of the cutting thickness and established a theoretical model for surface roughness under precision cutting conditions [13]:

$$R_Z = \frac{f^2}{8r_\varepsilon} + \frac{h_{min}}{2}\left(1 + \frac{r_\varepsilon h_{min}}{f^2}\right) \qquad (7)$$

Where: f is the feed rate, mm/r; rε is the tool nose radius, mm. After years of experimental verification, the Brammertz model has been proven to be in good agreement with experimental results. An analysis of the model reveals the following: when the feed rate and tool nose radius are fixed, the surface roughness

Journal of Manufacturing Engineering, September 2026, Vol. 21, Issue. 3, pp 117-128
DOI. https.//doi.org/10.37255/jme.v21i3pp117-128

increases as the minimum cutting thickness increases; when the feed rate is relatively large, the minimum cutting thickness has a negligible effect on the surface roughness; however, when the feed rate and the minimum cutting thickness are of the same order of magnitude, the influence becomes significant. Therefore, when selecting appropriate process parameters, they should be compatible with the corresponding minimum cutting thickness. According to the Brammertz model, if the cutting thickness is greater than the minimum cutting thickness, the surface roughness will increase; if the cutting thickness is less than the minimum cutting thickness, no chips will be generated, and the plowing effect of the cutting tool will be enhanced, leading to a significant deterioration in surface quality. Thus, only when the actual cutting thickness exceeds the minimum cutting thickness can good surface quality be expected.

Therefore, accurately determining the actual cutting thickness is crucial. Generally, for free cutting, the cutting thickness is considered to be equal to the feed rate [1,25], or

$$h = \sin K_r \qquad (8)$$

In actual production, the vast majority of cases involve non-free cutting. For a tool with a rounded nose, a typical non-free-cutting scenario is illustrated in Fig. 11. Reference [26] presents a calculation method for the cutting thickness, as given in Equation (9).

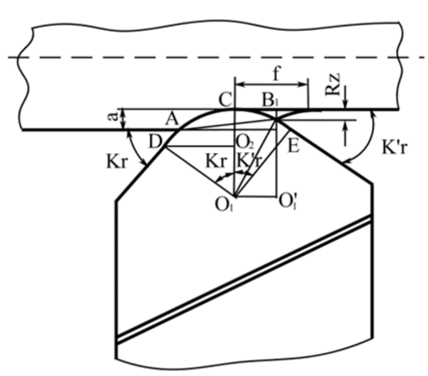

Fig. 11. Cutting Thickness in Non-free Cutting

Cutting Thickness in Non-free cutting,

$$= \frac{f}{c'} \sin \tan^{-1} \frac{c'}{\sqrt{2a'-1+a'b'}} \qquad (9)$$

$a' = \frac{r}{a}$, $b' = \frac{f}{2r}$, $c' = 1 - a'\left(1 - \sqrt{1 - b'^2}\right)$, r is the tool nose radius, a is the cutting depth, f is the feed rate, and h is the actual cutting thickness.

By referring to Equation (9), the relationship between the cutting thickness, the feed rate, and the ratio r/a is obtained, as shown in Fig. 12.

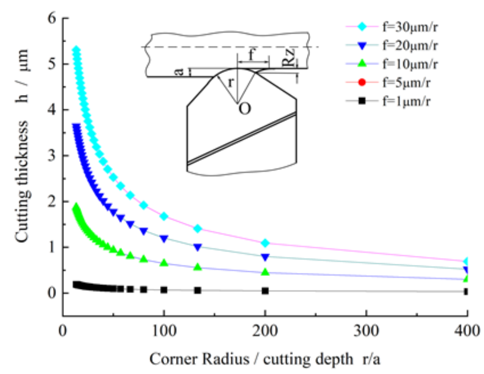

Fig. 12. Variation of Cutting Thickness with Feed Speed and Cutting Depth

As shown in Fig. 12, both the feed rate and the ratio r/a have a significant impact on the cutting thickness: the cutting thickness increases with increasing feed rate and decreases significantly with increasing r/a. Calculations show that: For aluminum alloy, with a minimum cutting thickness ranging from 2.2 μm to 3.17 μm, the corresponding feed rate is 15–22 μm/r when the cutting depth is 0.02 mm; For red copper, with a minimum cutting thickness ranging from 2 μm to 3.5 μm, the corresponding feed rate is 14–24 μm/r when the cutting depth is 0.02 mm. From this, the corresponding machining parameters for aluminum alloy and red copper are presented in Table 3.

Table 3: Processing Parameters for Aluminum Alloy and Red Copper

	Cutting speed n / r/min	Cutting depth a / mm	Feed speed f / μm/r
Aluminum alloy	800	0.02	15-35
Red copper	800	0.02	15-35

Cutting experiments on aluminum alloy and red copper were conducted using the parameters in Table 3, and the surface roughness was measured as shown in Fig. 13.

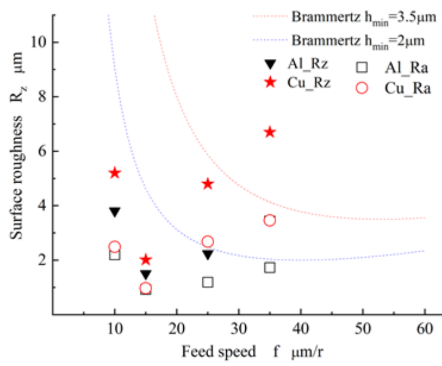

Fig. 13. Variation of Surface Roughness of Aluminum Alloy and Red Copper with Cutting Thickness

As shown in Fig. 13, when the feed rate is 15 μm/r, both aluminum alloy and red copper achieve their minimum surface roughness values: Rz = 1.505 μm and 2.014 μm, and Ra = 0.293 μm and 0.309 μm, respectively. When the feed rate is below 15 μm/r, numerous burrs are observed on the machined surfaces of both aluminum alloy and red copper. This is a typical characteristic of plowing cutting, which causes a sharp increase in the surface roughness of both materials. When the feed rate exceeds 15 μm/r, the surface roughness of the aluminum alloy increases relatively slowly, whereas that of red copper increases sharply. Both materials exhibit a "high at both ends and low in the middle" pattern, which is consistent with the variation trend of the Brammertz model. However, at lower feed rates, the experimental results are lower than the predicted values of the Brammertz model

5. Conclusions

Aluminum alloy and red copper were cut using a single-crystal diamond tool, and the sudden change in cutting force during the transition from plowing to cutting was measured. Based on this, the minimum cutting thickness was determined. The results show that as cutting speed increases, the ratio of the minimum cutting thickness of aluminum alloy to the cutting-edge radius increases slowly, with a variation range of 0.243–0.271. The ratio of the minimum cutting thickness of red copper to the cutting-edge radius increases relatively rapidly, with a variation range of 0.20091–0.36109 and an increase rate of nearly 80%. Furthermore, by utilizing the relationship between cutting thickness, feed rate, and cutting depth, the feed rate compatible with the minimum cutting thickness was obtained. This parameter was then used to cut aluminum alloy and red copper, and good surface quality was achieved at the feed rate corresponding to the minimum cutting thickness.

References

[1]. *Ikawa, N., Shimada, S., and Tanaka, H., "Minimum thickness of cut in micromachining," Nanotechnology, vol. 3, no. 1, pp. 6–9, 1992.*

[2]. *Shimada, S., Ikawa, N., Tanaka, H., et al., "Feasibility study on ultimate accuracy in microcutting using molecular dynamics simulation," CIRP Annals, vol. 42, no. 1, pp. 91–94, 1993.*

[3]. *Yuan, Z. J., Zhou, M., and Dong, S., "Effect of diamond tool sharpness on minimum cutting thickness and cutting surface integrity in ultraprecision machining," Journal of Materials Processing Technology, vol. 62, no. 4, pp. 327–330, 1996.*

[4]. *Son, S. M., Lim, H. S., and Ahn, J. H., "Effects of the friction coefficient on the minimum cutting thickness in micro cutting," International Journal of Machine Tools and Manufacture, vol. 45, nos. 4–5, pp. 529–535, 2005.*

[5]. *Zhang, H. L., Kuai, J. C., and Zhang, F. H., "Minimum thickness of cut in nanomachining using atomic force microscopy," in Proc. 2010 Int. Conf. E-Product E-Service and E-Entertainment (ICEEE), IEEE Conference Publishing, pp. 1276–1279, 2010.*

[6]. *Zhi, C. N., Fei, F. J., and Kai, C., "An innovative investigation on chip formation mechanisms in micro-milling using natural diamond and tungsten carbide tools," Journal of Manufacturing Processes, vol. 31, pp. 382–394, 2018.*

[7]. *Xian, W., Li, L., Ming, Y. D., Jian, Y. S., Feng, J., Yuan, L., and Yi, Y. L., "Experimental study on the minimum undeformed chip thickness based on effective rake angle in micro milling," Micromachines, vol. 11, p. 924, 2020.*

[8]. *Zhenyu, S., Yu, C. L., Zhan, Q. L., and Yang, Q., "Determination of minimum uncut chip thickness during micro-end milling Inconel 718 with acoustic emission signals and FEM simulation," International Journal of Advanced Manufacturing Technology, vol. 98, pp. 37–45, 2018.*

[9]. *Wojciechowski, S., "Estimation of minimum uncut chip thickness during precision and micro-machining processes of various materials—A critical review," Materials, vol. 15, p. 59, 2022, doi: 10.3390/ma15010059.*

[10]. *Lane, B. M., Dow, T. A., and Scattergood, R., "Thermo-chemical wear model and worn tool shapes for single-crystal diamond tools cutting steel," Wear, vol. 300, pp. 216–224, 2013.*

[11]. *Shi, Q. L., Hai, J. Z., Liang, Z., et al., "Coupled thermo-mechanical sticking-sliding friction model along tool-chip*

interface in diamond cutting of copper," Journal of Manufacturing Processes, vol. 70, pp. 578–592, 2021.

[12]. *Wan, Q. C., De, H. H., Xiang, Y. T., et al., "Surface generation modelling for micro end milling considering the minimum chip thickness and tool runout," Procedia CIRP, vol. 58, pp. 364–369, 2017.*

[13]. *Grzesik, W., "A revised model for predicting surface roughness in turning," Wear, vol. 194, no. 1, pp. 143–148, 1996.*

[14]. *Liu, X., Devor, R. E., and Kapoor, S. G., "An analytical model for the prediction of minimum chip thickness in micromachining," Journal of Manufacturing Science and Engineering, vol. 128, no. 2, pp. 474–481, 2006.*

[15]. *Özel, T., Liu, X., and Dhanorker, A., "Modelling and simulation of micro-milling process," in Proc. 4th Int. Conf. and Exhibition on Design and Production of Machines and Dies/Molds, Cesme, Turkey, Jun. 21–23, 2007.*

[16]. *Malekian, M., Mostofa, M. G., Park, S., and Jun, M. B. G., "Modeling of minimum uncut chip thickness in micro machining of aluminum," Journal of Materials Processing Technology, vol. 212, pp. 553–559, 2012.*

[17]. *Cuba Ramos, H., Autenrieth, T., Strauß, M., Deuchert, J., Hoffmeister, V., and Schulze, V., "Characterization of the transition from ploughing to cutting in micro machining and evaluation of the minimum thickness of cut," Journal of Materials Processing Technology, vol. 212, pp. 594–600, 2012.*

[18]. *Przestacki, D., Chwalczuk, T., and Wojciechowski, S., "The study on minimum uncut chip thickness and cutting forces during laser-assisted turning of WC/NiCr clad layers," International Journal of Advanced Manufacturing Technology, vol. 91, pp. 3887–3898, 2017.*

[19]. *Rezaei, H., Sadeghi, M. H., and Budak, E., "Determination of minimum uncut chip thickness under various machining conditions during micro-milling of Ti-6Al-4V," International Journal of Advanced Manufacturing Technology, vol. 95, pp. 1617–1634, 2018.*

[20]. *Yip, W. S. and To, S., "Reduction of minimum cutting thickness of titanium alloys in micro cutting by a magnetic field assistance," IEEE Access, vol. 7, pp. 152034–152041, 2019.*

[21]. *Mikołajczyk, T., Latos, H., Pimenov, D. Y., et al., "Influence of the main cutting edge angle value on minimum uncut chip thickness during turning of C45 steel," Journal of Manufacturing Processes, vol. 57, pp. 354–362, 2020, doi: 10.1016/j.jmapro.2020.06.040.*

[22]. *Mikołajczyk, T., Latos, H., Szczepaniak, Z., et al., "Theoretical and experimental research of edge inclination angle effect on minimum uncut chip thickness in oblique cutting of C45 steel," International Journal of Advanced Manufacturing Technology, vol. 124, nos. 7–8, pp. 2299–2312, 2023.*

[23]. *Yi, Q. L., Zhan, J. Y., Jin, K. X., Xiao, Z. L., and Hua, D. Y., "An analytical model for micro-cutting considering the cutting tool edge radius effect and material separation," International Journal of Advanced Manufacturing Technology, vol. 114, pp. 97–105, 2021.*

[24]. *Zhe, J. Y. and Xian, K. W., Precision and Ultraprecision Machining Technology. Beijing, China: China Machine Press, 2016.*

[25]. *Zhan, Q. L., Zhen, Y. S., and Yi, W., "Definition and determination of the minimum uncut chip thickness of microcutting," International Journal of Advanced Manufacturing Technology, vol. 69, nos. 5–8, pp. 1219–1232, 2013, doi: 10.1007/s00170-013-5109*